Nucl. Sci. and Tech., Vol.13, No. 2 (2023), pp. 47-55

Nuclear Science and Technology

Journal homepage: http://jnst.vn/index.php/nst

Wide-Aperture Backscattering Detector (BSD-A) for The High-Resolution Fourier Diffractometer

C.V. Hai[1, 5,*], A.M. Balagurov[1], A.A. Bogdzel[1], V.I. Bodnarchuk[1], O. Daulbaev[1, 3, 4], V.A. Drozdov[1], V.V. Zhuravlev[1], A.S. Kirilov[1], S.A. Kulikov[1], A.K. Kurilkin[1], A.A. Kazliakouskaya[1], V.M. Milkov[1], S.M. Murashkevich[1], M.M. Podlesnyy[1, 2], V.I. Prikhodko[1], M.O. Petrova[1], S.V. Sumnikov[1], A.V. Churakov[1] and V.V. Shvetsov[1]

[1] *Joint Institute for Nuclear Research (JINR), Dubna, Moscow region, 141980, Russian Federation*
[2] *Moscow Institute of Physics and Technology (National Research University), Dolgoprudny, Moscow region,141701, Russian Federation*
[3] *The Institute of Nuclear Physics, Ministry of Energy of the Republic of Kazakhstan, 050032 Almaty, Kazakhstan*
[4] *Al-Farabi Kazakh National University, 050038 Almaty, Kazakhstan*
[5] *Dalat University, Dalat, Lamdong province, Vietnam*
**E-mail: hajcao10@gmail.com*

Abstract: The high-resolution Fourier diffractometer (HRFD) has been in routine operation since 1994 at the long-pulse neutron source, the IBR-2 reactor, in Dubna. Its fast Fourier chopper provides probably the best compromise between very high resolution in reciprocal space ($\Delta d/d \approx 0.001$) and the intensity. For further improving intensity of TOF-diffraction pattern, a wide-aperture ring backscattering detector (BSD) has been developed on the basis of ZnS(Ag)/^{6}LiF scintillator. BSD is designed in the form of 6 concentric rings, each of which is subdivided into 12 identical parts. The main parameters of the detector are the following: range of scattering angles is 2θ = (133 - 175) degrees, covered solid angle is $\Omega_d \approx 2.0$ sr, average percentage absorption efficiency gets closer to 85%, geometrical contribution to resolution function does not exceed $\Delta d/d$ = 0.0005. In the report the concept of the detector is described and its data acquisition system is presented. The start of operation of the detector at the HRFD is scheduled for 2024.

Keywords: *Neutron diffraction, Fourier diffractometry, neutron detectors, detector electronics.*

I. INTRODUCTION

The High-Resolution Fourier Diffractometer (HRFD) developed as a part of collaborative effort of FLNP JINR (Dubna), PNPI (Gatchina) and VTT (Espoo, Finland) has been operating at the IBR-2 reactor since 1994. Its initial design, the principle of operation and nominal parameters are described in detail in [**1**]. The examples of numerous studies carried out with HRFD and the ideas on the possible development of the diffractometer are presented in [**2, 3**]. In the past few years some of the obsolete or worn-out key units have been replaced. Particularly, in 2016 a new mirror neutron guide and fast Fourier chopper were put into operation and before that a complete replacement in the diffraction spectra accumulation and experiment control electronics had taken place. The current status of HRFD is described in [**4**]. At present, the key element of the program for further modernization of HRFD is the replacement of existing backscattering detectors with their new version.

II. THE MAIN PART OF REPORT

Any modern high-resolution neutron diffractometer is a complex and expensive instrument, therefore precision neutron diffraction experiments with a very high resolution (at a level of $\Delta d/d \approx 0.002$ or higher) are currently carried out only in a few

https://doi.org/10.53747/nst.v13i2.421
Received 08 September 2023, accepted 07 November 2023

most advanced neutron laboratories in the world, including FLNP JINR, Dubna. Moreover, the HRFD diffractometer at the IBR-2 reactor is one of a few neutron diffraction instruments in the world where it is possible to conduct experiments requiring the resolution of $\Delta d/d \approx 0.001$ or higher. HRFD is mainly intended for the precision structural analysis of polycrystalline substances with an average unit cell volume of up to ~500 Å^3. Typical examples are the studies on mercury-based high-temperature superconductors with different concentrations of oxygen or fluorine in the basis plane [**5, 6**], the doped manganites with colossal magnetoresistance [**7, 8**], electrode materials [**9**] and Fe-based functional alloys [**10**]. HRFD is also used to perform an analysis of single crystals when its unique d_{hkl} resolution is needed, e.g., to study phase separation in La_2CuO_{4+6} crystals due to low-temperature diffusion of hyperstoichiometric oxygen [**11**]. The layout of HRFD at the IBR-2 reactor is presented in **Fig. 1.**

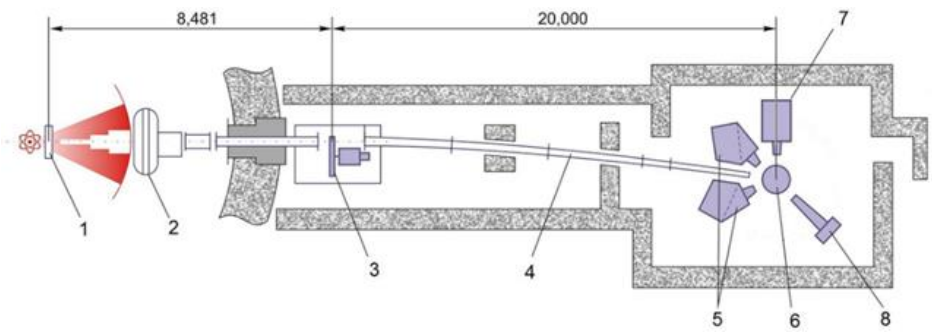

Fig. 1. The layout of the HRFD at the IBR-2 reactor (distances in mm): 1 - water moderator, 2 - background chopper, 3 - Fourier chopper, 4 – neutron guide, 5 – backscattering detectors, 6 – sample position, 7 - 90°-detector, 8 – position-sensitive detector at low scattering angle

At present the HRFD detector system consists of three detectors, two of which are located at scattering angles of ±152°, and the third one is at 90°. The first two detectors are mainly used for studying the structure of polycrystals and the third one is employed for measuring internal stresses. The detecting element is ^{6}Li-glass-based scintillators. From the contemporary perspective the HRFD detectors have two disadvantages: high sensitivity to the γ-background and an insufficiently large solid angle (~0.16 sr). It follows that the resulting diffraction spectra have a rather high background and low (by modern criteria) data set rate, even though the neutron flux at the sample position is sufficiently high (10^7n/cm^2/s).

The current project is aimed at eliminating the above stated drawbacks. Its implementation will allow us to radically improve the parameters of the HRFD diffractometer and make it the world leading.

The estimates show that diffraction spectrum obtained with the TOF diffractometer POWGEN3 (SNS/ORNL, $\Delta d/d \approx 0.001$) due to a large-area ZnS(Ag)-based detector (the solid angle covered by the detector is 1.5 sr) will have a low background and ~10 times better statistics than the spectrum from the same sample measured using HRFD. The solution for these problems will allow an approximately two- to three-fold increase in the number of conducted experiments, and in this respect will make it possible to substantially improve the accuracy of the obtained structural information, as well as to significantly enhance the capabilities of the diffractometer in performing experiments when various external influences are set on the sample.

A. Description of the new wide-aperture backscattering detector (BSD)

The detector comprises 6 ring assemblies of ZnS(Ag)/^{6}LiF-scintillation screens. The three inside rings are divided into 12 sectors, 30

degrees each part, and the three outside rings in each sector are further divided into 2 parts, covering 15 degrees. Six rings completely cover the scattering angle interval 2θ=(133-175)º. The total solid angle of the detector is $\Omega_D \approx 2.0$ **sr**. The design of BSD is schematically shown in **Fig. 2** [**12**], and **Fig. 3** shows photographs of the assembly of the detector housing.

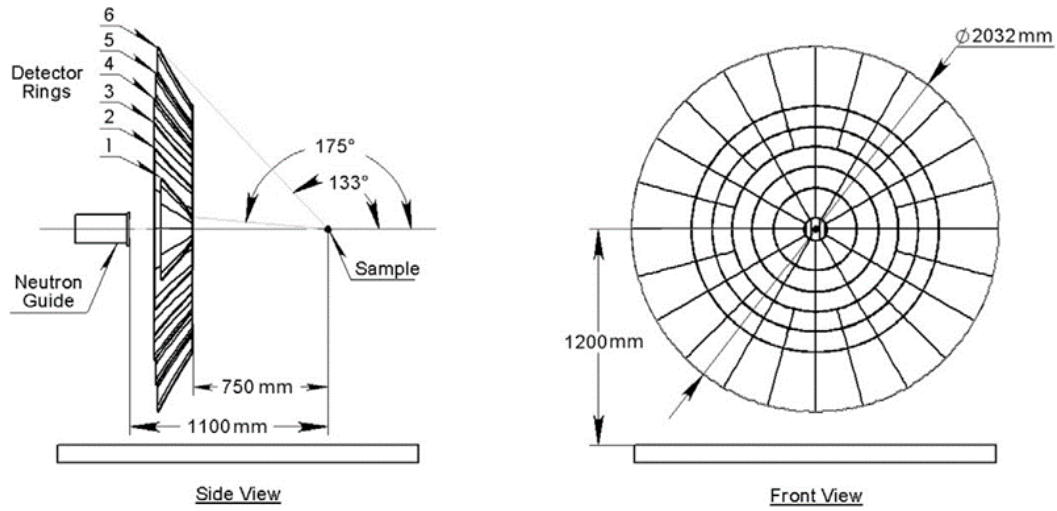

Fig. 2. Scheme of the large-aperture backscattering detector

Fig. 3. Assembly of the BSD housing

Each sector represents a separate detector element of a photomultiplier, a wavelength-shifting (WLS) fiber for light collection, and a scintillation screen. The detector is built on a thin ZnS(Ag)/^{6}LiF scintillation screen that is 0.42 mm thick (2:1 ^{6}LiF ratio by weight). Optical WLS fibers are adhered to both sides of the scintillator to collect and transmit light from scintillation screens to photomultipliers. ZnS(Ag)/^{6}LiF scintillation screen application features are thoroughly described in [**13**]. The scintillation screen in each ring is divided into smaller, identical fragments (elements) that fit tightly together and precisely follow the contours of the space-time focusing surface of the detector

(**Fig. 4**). The output of each photomultiplier is connected to the Data Acquisition and Accumulation (DAQ) System developed at the Laboratory. The System components are described in detail in [**14, 15, 16**]. The system allows to receive and process information from 240 independent detectors, suppressing the events caused by background gamma-rays. The system is designed according to the NIM standard. In its full configuration, it consists of 8 units of amplifiers-discriminators with 32 inputs each and one data accumulation unit.

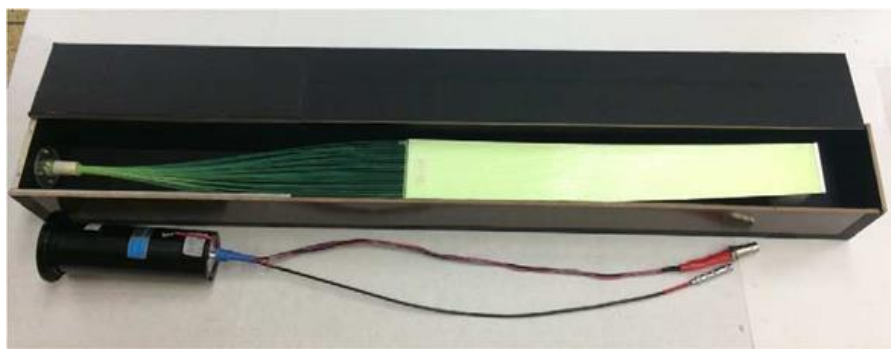

Fig. 4. One assembled detector element

The shape of the detector elements of all 6 rings meets the space-time focusing condition. The rotation surfaces which elements are shown in **Fig. 5**. are perfect for the space-time focusing.

The main geometric characteristics of the detector rings, providing guidance on its position at the HRFD diffractometer are shown in **Table I**.

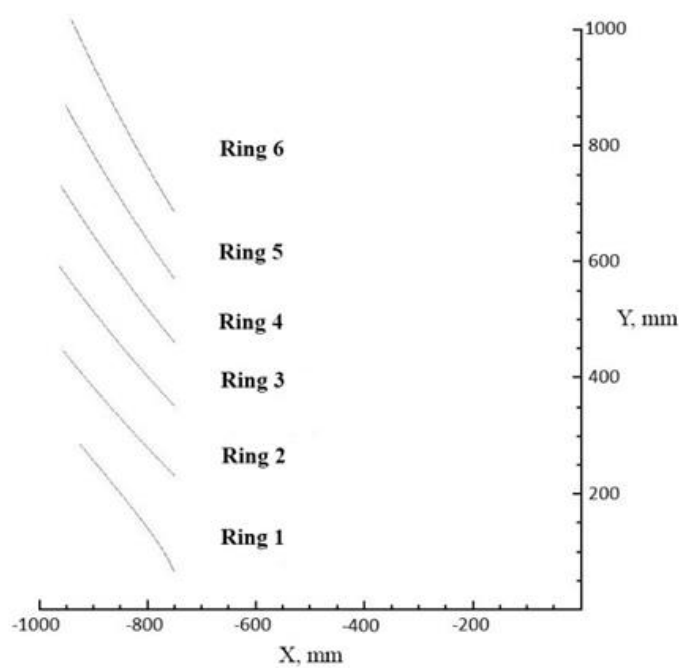

Fig. 5. Shape of the detector elements of the rings

Table I. Main geometric characteristics of the backscattering detector rings:

Quantity	Ring №1	Ring №2	Ring №3	Ring №4	Ring №5	Ring №6
θ_{max}, °	175.047	162.913	154.917	148.417	142.721	137.547
θ_{min}, °	162.913	154.917	148.417	142.721	137.547	132.745

l, mm	280	300	320	340	360	380
X_{max}, mm	-750.00	-750.00	-750.00	-750.00	-750.00	-750.00
Y_{max}, mm	65.00	230.55	351.05	461.10	570.91	686.12
X_{min}, mm	-923.44	-956.79	-961.40	-958.44	-950.62	-938.82
Y_{min}, mm	283.86	447.84	591.07	729.58	869.65	1015.77
ΔΩ, sr	0.02117	0.02627	0.02818	0.01471	0.01515	0.01547
Ω, sr	0.25388	0.31518	0.33814	0.35300	0.36360	0.37127

$\theta_{max}, \theta_{min}$ – maximum and minimum scattering angles, which are covered by the ring; l – length of the detector elements in **Fig. 5**; $X_{max}, X_{min}, Y_{max}, Y_{min}$ – coordinates of the end points of the scintillation screen of each ring; ΔΩ – solid angle covered by one sector of the ring; Ω – total solid angle covered by the ring.

The dependence of the effective thickness of the detector (d_{eff}) on the scattering angle, i.e. the thickness that the neutron scattered on the sample encounters, is shown in **Fig. 6**. This thickness determines both the detector efficiency and contribution to the geometric component of the diffractometer resolution.

The effective thickness calculations are based on the actual thickness of the scintillation screen of 0.42 mm, which is optimal in terms of the balance between efficiency and transparency.

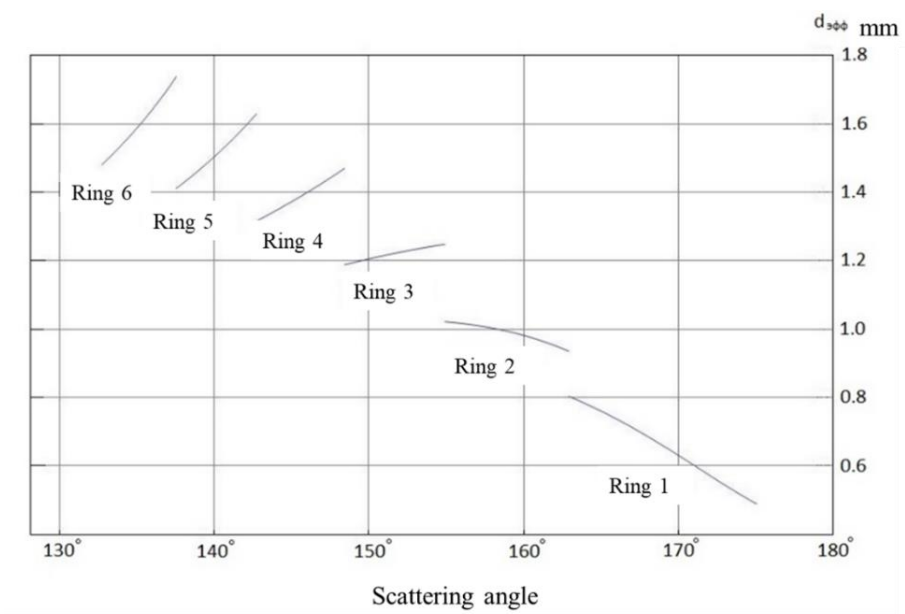

Fig. 6. Dependence of the detector effective thickness (d_{eff}) on the scattering angle. Thickness of the scintillation screen is 0.42 mm

The geometric contribution to the total resolution was evaluated considering only the effective thickness of the detector and various sizes of the sample ranging from 1 mm to 8 mm $\emptyset_{samp}$ studied on the diffractometer. As it was assumed, the shape of the scintillation screen exactly corresponds to the shape of the time focusing surface and the initial divergence of the neutron beam is zero. The results of this evaluation are presented in **Table II**, showing that for the chosen detector geometry the contribution from the thickness of the scintillation screen and from the sample size to the total resolution of the diffractometer is significantly lower than the allowable value (0.001). The technological and technical solutions currently used at the Laboratory make it possible to provide the shape of the screen corresponding to the time focusing surface with the required accuracy.

Table II. Geometric contribution to the total resolution of the diffractometer. $\emptyset_{samp}$ – sample size; $< \Delta_i >= 2.36\sigma_i$– error value for the i-th ring of the detector

$\emptyset_{обр}$, мм	1	2	3	4	5	6	7	8
$< \Delta_1 >$	4.0×10^{-5}	6.9×10^{-5}	1.0×10^{-4}	1.3×10^{-4}	1.7×10^{-4}	2.0×10^{-4}	2.3×10^{-4}	2.6×10^{-4}
$< \Delta_2 >$	4.6×10^{-5}	7.3×10^{-5}	1.0×10^{-4}	1.3×10^{-4}	1.7×10^{-4}	2.0×10^{-4}	2.3×10^{-4}	2.6×10^{-4}
$< \Delta_3 >$	5.1×10^{-5}	7.6×10^{-5}	1.1×10^{-4}	1.4×10^{-4}	1.7×10^{-4}	2.0×10^{-4}	2.3×10^{-4}	2.6×10^{-4}
$< \Delta_4 >$	5.5×10^{-5}	7.9×10^{-5}	1.1×10^{-4}	1.4×10^{-4}	1.7×10^{-4}	2.0×10^{-4}	2.3×10^{-4}	2.6×10^{-4}
$< \Delta_5 >$	5.8×10^{-5}	8.1×10^{-5}	1.1×10^{-4}	1.4×10^{-4}	1.7×10^{-4}	2.0×10^{-4}	2.3×10^{-4}	2.6×10^{-4}
$< \Delta_6 >$	6.1×10^{-5}	8.2×10^{-5}	1.1×10^{-4}	1.4×10^{-4}	1.7×10^{-4}	2.0×10^{-4}	2.3×10^{-4}	2.6×10^{-4}

The dependence of the detector efficiency on the scattering angle, is presented in **Fig. 7** for one and two scintillator layers, calculated for a neutron wavelength of 1.8 Å using the effective thickness of the scintillator due to the location of the detecting surfaces at an angle to the incident neutron beam. The lower set of curves in the last figure corresponds to one scintillator layer. The detector efficiency in this case varies from 36% to 80% and on average it is 65%. To increase efficiency, a second layer of scintillator is added to each ring. As it can be seen from the upper set of curves in **Fig. 7**, the efficiency range becomes 59%-96% and on average it increases to 85%. This increase in efficiency, combined with the aperture increased to 2.0 sr, will bring the backscattering detector to a completely new level. The mechanical design of the detector with addition of the second layer remains practically unchanged.

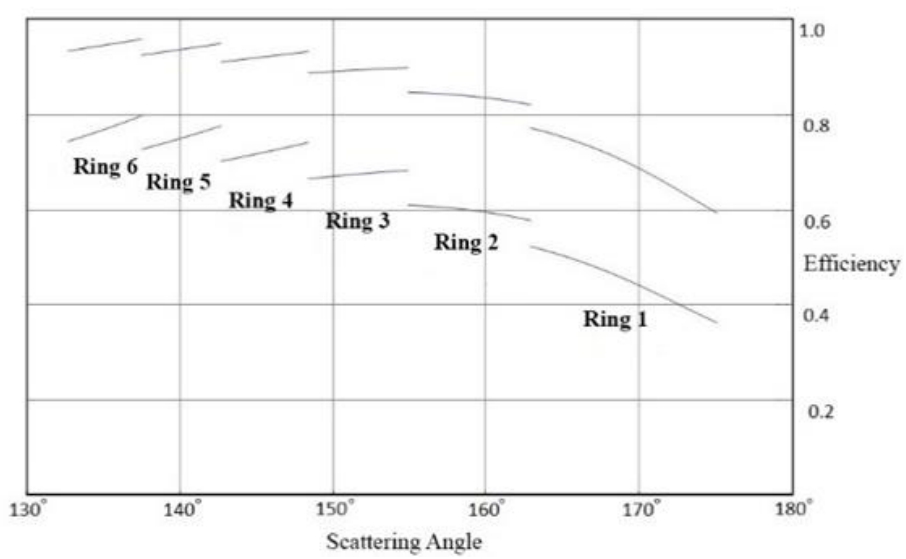

Fig. 7. Dependence of the detector efficiency on the scattering angle

B. Data acquisition electronics

The HRFD diffractometer currently uses a data acquisition system based on MPD-240 DAQ [**15**], this system, however, has a registration rate limit of 10^6 events/sec and is unable to provide high-resolution data acquisition for the detector that is currently under development. It is necessary to create a new, high-performance DAQ system with data transmission band channels capable of 200 MB/s. For this purpose, a new MPD-32 module has been developed at FLNP (**Fig. 8**) [**16**]. This module combines the functions of the 32-channel analog discriminator module of input detector signals and the encoder of their registration time. The signals from the detector elements are received at the inputs of the module, which, after the threshold

discrimination, generates logical signals and transmits them to the inputs of the time encoder of signals registration (TOF encoder). The digital part of the module also performs the functions of organizing communication in the integrated data acquisition system, including maintenance of the USB3.0 communication interface with a computer and inter-block communication interface for combining several modules into a single system with the required number of registered data channels. MPD-32 module main characteristics:

- MPD-32 system operates as a discriminator and a time recorder for 32 analog signals;

- Maximum registration rate is 3×10^7 events/sec;

- The events are recorded in the experiment absolute time; the exposure time limit is 4.5×10^6 seconds;

- Communication with the computer is realized via the USB3.0 interface;

- Inter-block communication is based on the 2.5 Gbps Fast Serial Link.

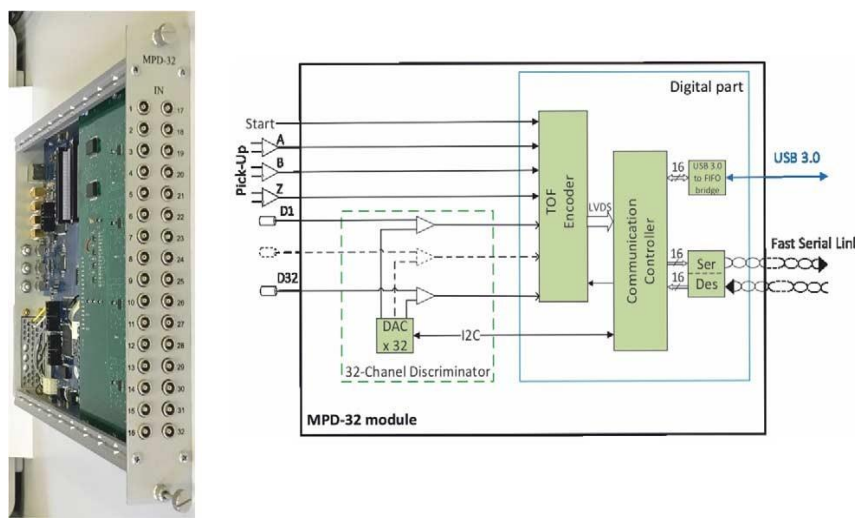

Fig. 8. Photo and block diagram of the MPD-32 module

A wide-aperture detector data acquisition device is possible to construct using 8 MPD-32 modules that are integrated into a device for registering signals from 216 PMTs (**Fig. 9**). The modules send data packages containing unit addresses, identification of signals with their registration times, and the digitization data of the detector signals, along with data on the pickup signals of the Fourier chopper, to the computer. The RTOF-method algorithm is used to further process the raw data collected during measurements on the Fourier diffractometer in an offline mode.

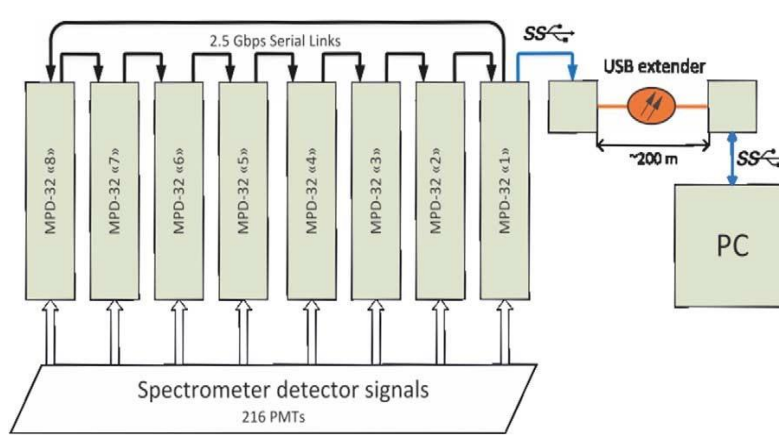

Fig. 9. MPD-32-based data acquisition system block diagram

III. CONCLUSIONS

The completion of work on this project will provide an opportunity to obtain a new world-class instrument, which will undoubtedly be in demand among researchers from both JINR and other organizations, including the foreign ones.

The new wide-aperture detector will allow to radically improve the parameters of HRFD. First, it concerns the luminosity of the diffractometer, which is supposed to be increased by about 10 times. This will allow to increase the number of conducted experiments by approximately two to three times, and in this respect will make it possible to substantially improve the accuracy of the obtained structural information, as well as to significantly enhance the capabilities of the diffractometer in performing experiments when various external influences are set on the sample.

The physical start of the detector at the HRFD facility is scheduled for 2024.

ACKNOWLEDGEMENTS

We would like to thank our colleagues V.A. Kudryashev (PNPI, Gatchina) and E.S. Kuzmin (JINR, Dubna) who participated in the development of the detector concept. This work was partly supported by the Russian Science Foundation (project no. 22-42-04404).

REFERENCES

[1]. Aksenov V.L., Balagurov A.M., Simkin V.G., Bulkin A.P. et al., “Performance of the high resolution Fourier diffractometer at the IBR-2 pulsed reactor” J. of Neutron Research, 1997, v.5, pp. 181-200. Препринт ОИЯИ, Р13-96-164, Дубна, 1996.

[2]. Balagurov A.M., “High resolution Fourier diffraction at the IBR-2 reactor” Neutron News, 16 (2005) 8-12.

[3]. Balagurov A.M., Kudrjashev V.A., “Correlation Fourier diffractometry for long-pulse neutron sources: a new concept” ICANS-XIX conference, 08-12.04.2010, Grindenwald, Switzerland.

[4]. Balagurov A.M., Balagurov D.A., Bobrikov I.A., Bogdzel A.A. et al., High-resolution neutron Fourier diffractometer at the IBR-2 pulsed reactor: a new concept. Nuclear Inst. and Methods in Physics Research B 436 (2018), pp.263-271

[5]. Aksenov V.L., Balagurov A.M. , Sikolenko V.V., Simkin V.G. et al., “Precision neutron diffraction study of the high-T_c superconductor $HgBa_2CuO_{4+\delta}$” *Phys. Rev. B*, 1997, v.55, pp.3966-3973.

[6]. Abakumov A.M., Aksenov V.L., Antipov E.V., Balagurov A.M. et al., “Effect of fluorination on the structure and superconducting properties of the Hg-1201 phase” *Phys. Rev. Lett.*, 1998, v.80(2), pp.385-388.

[7]. Balagurov A.M., Pomjakushin V.Yu., Sheptyakov D.V., Aksenov V.L. et al., “Effect of oxygen isotope substitution on magnetic structure of $(La_{0.25}Pr_{0.75})_{0.7}Ca_{0.3}MnO_3$” *Phys. Rev. B*, v.60(1), 1999, pp.383-387.

[8]. Balagurov A.M., Pomjakushin V.Yu., Sheptyakov D.V., Aksenov V.L. et al., “A-cation size and oxygen isotope substitution effects on $(La_{1-y}Pr_y)_{0.7}Ca_{0.3}MnO_3$ structure” *Eur. Physical J. B*, 2001, v. 19 (2), pp.215-223.

[9]. Golovin I.S., Balagurov A.M., Palacheva V.V., Bobrikov I.A. et al., In situ neutron diffraction study of bulk phase transitions in Fe-27Ga alloys, Materials and Design 98 (2016) 113-119

[10]. Bobrikov I.A., Balagurov A.M., Chih-Wei Hu, Chih-Hao Lee et al., Structural evolution in $LiFePO_4$-based battery materials: in-situ and ex-situ time-of-flight neutron diffraction study, Journal of Power Sources 258, 356-364 (2014)

[11]. Balagurov A.M., Pomjakushin V.Yu., Simkin V.G., Zakharov A.A. “Neutron diffraction study of phase separation in La_2CuO_{4+y} single crystals” *Physica C*, 1996, v.272, pp.277-284.

[12]. Kruglov V.V., Balagurov A.M., Belova M.O., Bobrikov I.A., Bogdzel A.A., Bodnarchuk V.I., Bulavina V.V., Daulbaev O., Drozdov V.A., Zhuravlev V.V., Kirilov A.S., Kulikov S.A., Kurilkin A.K., Milkov V.M., Murashkevich S.M., Podlesnyy M.M., Prikhodko V.I., Churakov A.V. and Shvetsov V.V. “Wide-aperture back-scattering detector (BSD) for the High-Resolution Fourier Diffractometer

(HRFD) at the IBR-2 reactor", Journal of Neutron Research 23 (2021) 243–250.

[13]. E.S. Kuzmin, A.M. Balagurov, G.D. Bokuchava, V.V. Zhuk, V.A. Kudryashev, A.P. Buklin and V.A. Trounov, Detector for the FSD Fourier Diffractometer based on ZnS(Ag)/6LiF Scintillation Screen and Wavelength shifting Fibers Readout, Journal of Neutron Research (2002), 31–41. doi:10.1080/10238160290027748.

[14]. Levchanovskiy F.V., Murashkevich S.M. "The Data Acquisition System for Neutron Spectrometry – a New Approach and Implementation", NEC'2013, pp.176-179.

[15]. Shvetsov V.V., Drozdov V.A.. "Increasing Bandwidth of Data Acquisition Systems on IBR-2 Reactor Spectrometers in FLNP". Proceedings of the XXVI International Symposium on Nuclear Electronics & Computing (NEC'2017) Becici, Budva, Montenegro, September 25 - 29, 2017, European repository of the CEUR Workshop Proceedings Vol-2023, pp. 293-298.

[16]. Bogdzel A., Drozdov V., Kruglov V., Murashkevich S., Prikhodko V. Shvetsov V., «The new data acquisition system MPD-32 for the high-resolution Fourier diffractometer at the IBR-2 pulsed reactor». Proceedings of the 27th International Symposium Nuclear Electronics and Computing (NEC'2019) Budva, Becici, Montenegro, September 30–October 4, 2019, CEUR-WS Vol-2507 (ISSN 1613-0073), pp.142-146 (https://indico.jinr.ru/event/738/contributions/6365/).